representation of the shock front become necessary, Lewis et al. (1984) have devised a nodal discontinuity technique which accurately represents and predicts the shock front movement.

REFERENCES

Bettencourt, J.M., Zienkiewicz, O.C. and Cantin, G., 1981. Consistent use of finite elements in time and the performance of various recurrence schemes for the heat diffusion equation. Int. J. Numer. Meth. Engng, 17: 931–938.
Blandford, G.E. and Meadows, M.E., 1984. Finite element simulation of kinematic surface runoff. In: J.P. Laible, C.A. Brebbia, W. Gray and G. Pinder (Editors), Finite Elements in Water Resources, Proc. 5th Int. Conf., Burlington, VT, June 1984. Springer-Verlag, New York, pp. 153–164.
Chow, V.T., 1959. Open-Channel Hydraulics. McGraw–Hill, New York, p. 8 and pp. 110–113.
Hughes, T.J.R., 1977. Unconditionally stable algorithms for nonlinear heat conduction. Comput. Meth. Appl. Mech. Engng, 10: 135–139.
Izzard, C.F., 1946. Hydraulics of runoff from developed surfaces. Highway Research Board, Proc. 26th Annual Meeting, University of Kentucky, pp. 129–150.
Jayawardena, A.W. and White, J.K., 1977. A finite element distributed catchment model, I: Analytical basis. J. Hydrol. 42: 231–249.
Kibler, D.F. and Woolhiser, D.A., 1972. Mathematical properties of the kinematic cascade. J. Hydrol. 15: 131–147.
[illegible] 973. Computational Methods in Ordinary Differential Equations, Wiley, New York.
Lewis, R.W., Morgan, K., Pugh, E.D.L. and Smith, T.J., 1984. A note on discontinuous numerical solutions of the kinematic wave motion. Int. J. Numer. Method. Engng, 20: 555–563.
Li, R.M., Simons, D.B. and Stevens, M.A., 1975a. Nonlinear kinematic wave approximation for water routing. Water Resour. Res., 11(2): 245–252.
Li, R.M., Simons, D.B. and Stevens, M.A., 1975b. On overland flow water routing. Nat. Symp. Urban Hydrology and Sediment Control, University of Kentucky, Lexington, KY, July 28–31, pp. 237–244.
Overton, D.E. and Meadows, M.E., 1976. Stormwater Modeling. Academic Press, New York, pp. 3–15.
Ross, B.B., Contractor, D.N. and Shanholtz, V., 1979. A finite element model of overland and channel flow for assessing the hydrologic impact of land-use change. J. Hydrol., 41: 11–30.
Schreiber, D.L. and Bender, D.L., 1972. Obtaining overland flow resistance by optimization. J. Hydraul. Div., ASCE, 98 (HY3): 429–446.
Shen, H.W. and Li, R.M., 1973. Rainfall effect on sheet flow over smooth surface. J. Hydraul. Div., ASCE, 99 (HY5): 771–792.
Viessman, W., Jr., Knapp, J.W., Lewis, G.L. and Harbaugh, T.E., 1977. Introduction to Hydrology, 2nd edn. Harper and Row, New York, p. 259.
Woolhiser, D.A. and Liggett, J.A., 1967. Unsteady one-dimensional flow over a planet – the rising hydrograph. Water Resour. Res., 3(3): 753–771.
Yu, Y.S. and McNown, J.S., 1964. Runoff from impervious surfaces. J. Hydraul. Res., 2(1): 2–24.

$km^3 = 10^9 m^3$ and $1233 m^3$ = ac-ft

$752 km^3 * 10^9 / 1233 = 600 \times 10^6$ ac-ft

Journal of Hydrology, 119 (1990) 357–388
Elsevier Science Publishers B.V., Amsterdam — Printed in The Netherlands

[2]

A DEUTERIUM-CALIBRATED GROUNDWATER FLOW MODEL OF A REGIONAL CARBONATE–ALLUVIAL SYSTEM

STEPHEN T. KIRK* and MICHAEL E. CAMPANA**

Water Resources Center, Desert Research Institute, P.O. Box 60220, Reno, NV 89506 (U.S.A.)

(Received March 22, 1989; accepted after revision December 16, 1989)

ABSTRACT

Kirk, S.T. and Campana, M.E., 1990. A deuterium-calibrated groundwater flow model of a regional carbonate–alluvial system. J. Hydrol., 119: 357–388.

The White River Flow System (WRFS), a regional carbonate–alluvial groundwater system in southeastern Nevada, U.S.A., contains large amounts of water in storage, especially in the underlying carbonate reservoir. As the population of Nevada grows, it may become necessary to tap the resources of this and other regional carbonate systems. Because of the depth to the carbonate reservoir and, until now, lack of motivation to collect detailed hydrogeological data on it, the state of knowledge of flow in the carbonate system is poor. However, a simple mixing-cell flow model of the WRFS can be constructed and calibrated with the spatial distribution of the stable isotope deuterium. This type of model subdivides the system into carbonate and alluvial cells and routes water and deuterium through the entire cell network. It provides estimates of recharge rates, groundwater ages and volumes of water in storage. Transience in recharge rates and their deuterium signatures are unaccounted for by the model.

The lack of constraints on the system mandates the calibration of three different flow scenarios, each of which differs slightly from the other. Despite these differences, some consistent quantitative results are obtained. Foremost among these are: (1) the carbonate aquifer may contain as much as 752 km^3 of water in storage; (2) recharge from the Sheep Range to Coyote Spring Valley is at least 90% greater than previously believed; (3) Lower Meadow Valley is part of the WRFS and contributes underflow to Upper Moapa Valley; (4) underflow with an average value of 0.163 $m^3 s^{-1}$ flows westward out of the system along the Pahranagat Shear Zone; (5) recharge to the alluvial system is greater than that to the carbonate system; (6) groundwater mean ages range from 1600 to 34 000 years, with the oldest waters exceeding 100 000 years old. The results also demonstrate that deuterium can be used to calibrate simple flow models and provide groundwater ages.

Despite the uncertainties and lack of constraints in mixing-cell models, they provide first approximations to information which, until now, has been difficult, if not impossible, to obtain. These models are especially useful for analyzing sparse-data systems, testing different flow hypotheses with minimal effort, providing ranges in parameter estimates, guiding future data collection and serving as precursors for the development of more sophisticated models.

* Present address: CH2M Hill, P.O. Box 91500, Bellevue, WA 98009, U.S.A.
** Present address: Department of Geology, University of New Mexico, Albuquerque, NM 87131, U.S.A.

0022-1694/90/$03.50

I[illegible]ON

Long-term water supply needs in southern and eastern Nevada, U.S.A., have rekindled interest in regional carbonate flow systems within the Paleozoic miogeosynclinal belt of eastern Nevada. This paper describes the quantification of various flow properties of one such system, the White River Flow System (WRFS), shown in Fig. 1. The WRFS was originally defined by Eakin (1966),

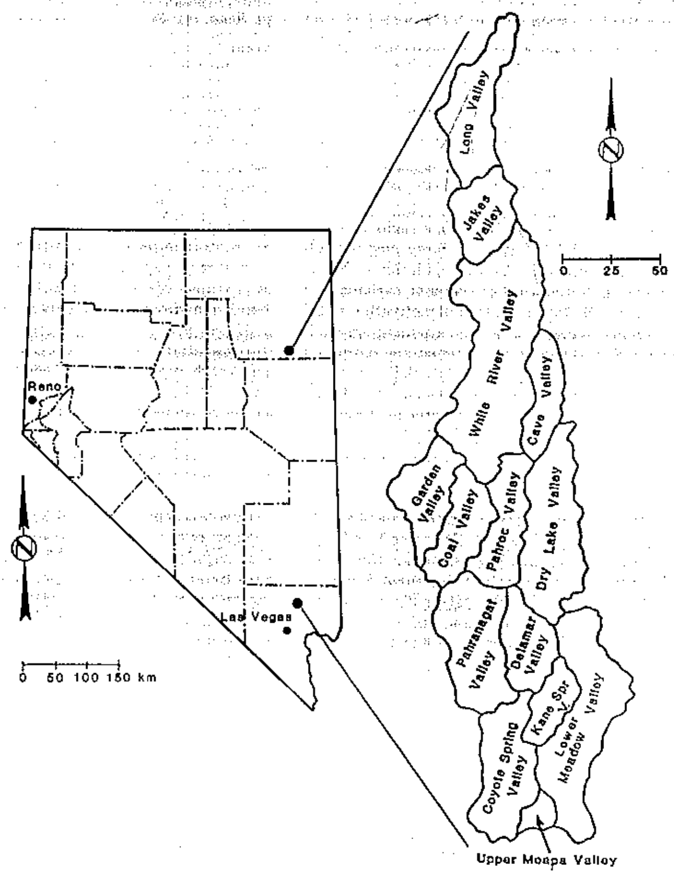

Fig. 1. Location of the White River Flow System.

who used a water-budget approach to delineate the system boundaries. Because of the areal extent of this flow system (20 000 km^2), sparse data, and uncertainties in the hydrogeological parameters (saturated thicknesses, porosities, and recharge volumes), it is difficult to use a conventional flow model to obtain quantitative estimates of the system's properties. However, a simple mixing-cell model, which requires fewer data, can yield estimates of storage volumes, groundwater residence times, and recharge rates. The application and hydrological implications of such a model vis-à-vis the WRFS are the subject of this investigation.

As originally defined by Eakin (1966), the WRFS includes thirteen topographic basins and extends 400 km from north to south, encompassing an area of > 18 000 km^2. Eakin's original flow system excluded Lower Meadow Valley, which is included in our model. The land surface slopes to the south, with valley floor elevations decreasing from 1700 m above mean sea level (msl) in the north to 550 m above msl in the vicinity of Muddy River Springs, the distal end of the system. In the northern part of the study area, the crests of the mountain ranges commonly exceed 2400 m in elevation and locally exceed 3000 m. In the southern part, mountain crests exceed 2400 m only locally and generally are < 2100 m above msl.

The objectives of this study were to:

(1) simulate flow in a large regional aquifer system using a simple mixing-cell model calibrated with the environmental stable isotope deuterium;

(2) use this model to estimate the aquifer system's storage volume, average annual recharge rates and flow distributions;

(3) document the ability of the stable isotope-calibrated model to estimate groundwater age distributions.

These objectives will be accomplished by use of three different flow scenarios, each of which may be feasible, given the lack of detailed hydraulic and hydrologic information on the WRFS.

GEOLOGY

The regional geology of the WRFS is dominated by Basin and Range horst and graben structure, formed by high-angle normal faults, oriented north–south. The intermontane basins (grabens) have been filled with alluvium eroded from the mount[illegible] blocks (horsts). As this stud[illegible] [illegible]ional groundwater flow, the [illegible] [illegible]cal descrip[illegible]

Exposed rocks in the WRFS generally fall into three grou[illegible] Precambrian to Triassic igneous, metamorphic, and sedimentary rocks; Cenozoic sedimentary rocks; and Cenozoic volcanic rocks. Paleozoic rocks belong to the carbonate or eastern assemblages which were formed in shallow marine, intertidal, and supertidal depositional environments (Stewart, 1980).

Mesozoic sedimentary rocks were eroded during the period from the late Triassic uplift to late Jurassic or Cretaceous thrust faulting. Throughout the Tertiary, a huge outpouring (perhaps 1000 km^3) of volcanic material occurred.

These Tertiary volcanic rocks, largely tuffs, are predominantly exposed in the southern half of the WRFS. Volcanism was followed by late Cenozoic Basin and Range faulting and deposition of valley-fill sediments (Tschanz and Pampeyan, 1970).

The geological structure of the region was formed by compression during the Mesozoic–early Tertiary Sevier Orogeny, and extension during the Miocene–Holocene. Normal faults underlying valleys of the WRFS can serve as areas of spring discharge. The WRFS is divided by a regional lineament, the Pahranagat Shear Zone, composed of a series of parallel northeast–southwest trending strike-slip faults. This zone, exposed in the Pahranagat Range, which forms the western boundary of Pahranagat Valley, is composed of distinct parallel faults: the Arrowhead Mine, Buckhorn, and the Maynard Lake Faults. Northeast–southwest trending lineaments have also been mapped in the Arrow Canyon Range at the southern end of the WRFS and identified as deep-seated structural anomalies which serve as conduits for regional groundwater flow (McBeth, 1986).

HYDROGEOLOGY

Hydrostratigraphy

Three distinct hydrostratigraphic units occur in the WRFS: (1) Paleozoic carbonates; (2) Tertiary volcanics; (3) Tertiary and Quaternary valley fill. A map of these rock types is shown in Fig. 2.

Large quantities of groundwater are known to flow through the Paleozoic carbonate rocks in eastern Nevada (Eakin, 1966). Transmissive properties of the Paleozoic carbonates are facilitated by secondary porosity as a result of faults, joints, fractures and solution channels (Hess and Mifflin, 1978). Locally, the stratigraphic section of the Paleozoic carbonates exceeds 9000 m (Kellog, 1963). Within these Paleozoic rocks are low-permeability clastic rocks, primarily quartzite and shale, which act as aquitards. Knowledge of the total thickness of the transmissive section of the Paleozoic carbonates and corresponding effective porosity is difficult to obtain because of the paucity of deep borehole data.

Tertiary volcanics are extensive in the region. The primary porosity of these rocks is low but secondary porosity exists, as a result of joints and fractures. In many places, Tertiary volcanics lie between Paleozoic carbonates and valley fill.

Valley-fill alluvium was deposited in the north–south trending grabens and is composed of fine-grained lacustrine or playa deposits or Quaternary gravels, sand, silts and clay laid down in stream channels, alluvial fans and playa environments. Unconsolidated sand and gravel deposits of the younger valley-fill and alluvial fans are capable of transmitting water freely (Eakin, 1966).

Thicknesses of valley-fill deposits vary greatly. In Coyote Spring Valley the average thickness of the valley fill is 100 m, whereas in Dry Lake Valley the estimated maximum thickness, based on gravity surveys, is 3000 m.

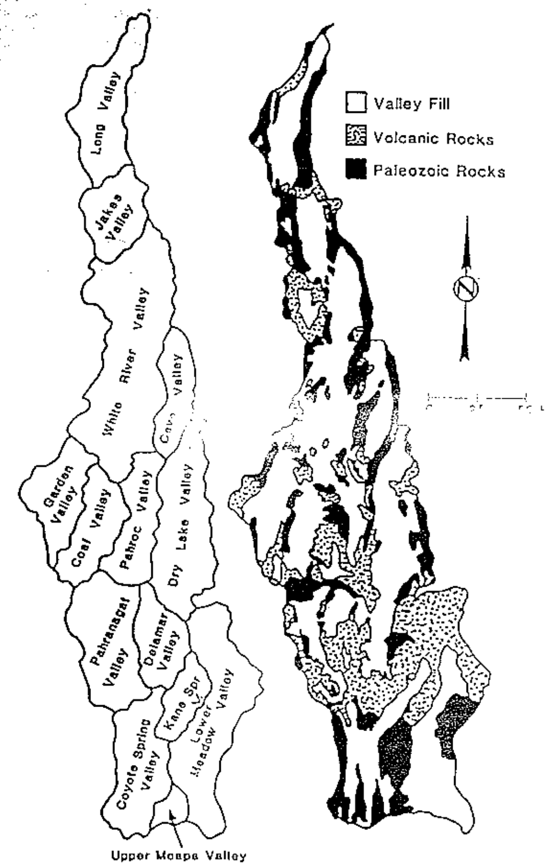

Fig. 2. Hydrostratigraphic units in the White River Flow System.

Groundwater

The occurrence of groundwater in the WRFS is generally confined to the three hydrostratigraphic units previously defined. Regional movement of groundwater in the WRFS was originally proposed by Eakin (1966), who based his conceptual model upon: (1) relative hydraulic properties of the major rock groups; (2) regional movement of groundwater as inferred from hydraulic gradients; (3) relative distribution and quantities of estimated recharge and discharge; (4) chemical quality of water discharged from major springs. Flow paths defined by Eakin are shown in Fig. 3; arrows indicate the general direction of groundwater flow.

In defining the boundaries of the WRFS, Eakin assumed that: (1) the mountain bedrock is virtually impermeable and lateral movement of water conforms to the general slope of the surface topography; (2) topographic axes of mountain ranges are coincident with structural trends which act as barriers to groundwater flow; (3) groundwater divides are coincident with topographic

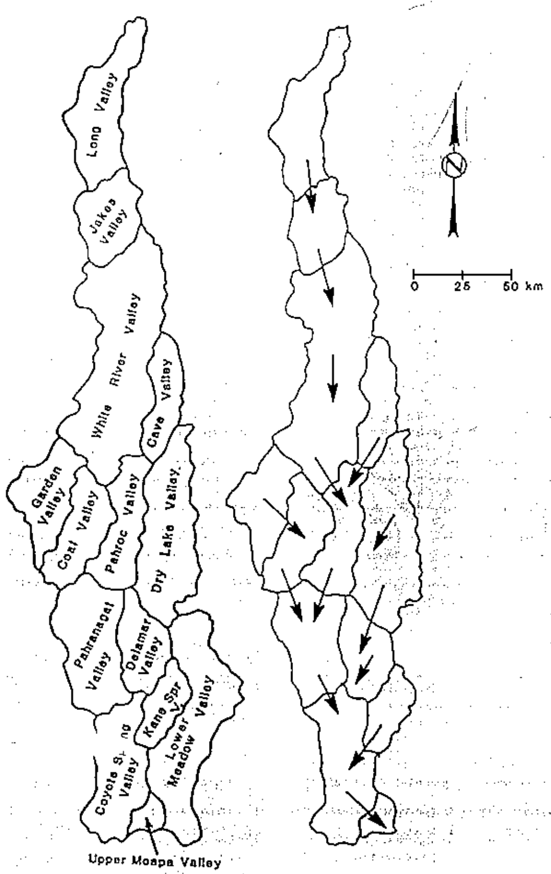

Fig. 3. Flow paths in the White River Flow System according to Eakin (1966).

$(3.28)^3$ ft^3 = 1 m^3
30 cfs & 19 cfs warm H$_2$O
cold H$_2$O
at White River Valley
or 35000 acft/yr

divides. The first and last assumptions can be in error for certain instances where hydraulic gradients in a regional aquifer are not coincident with those in the overlying alluvial aquifer and with the gradient of the topography. However, given the paucity of hydrologic data available to Eakin, his assumptions were reasonable. Horizontal hydraulic gradients were obtained from water levels in alluvial wells and springs. Eakin assumed that hydraulic gradients in the regional aquifer were somewhat less than in the overlying alluvial aquifer. Estimates of recharge volumes were obtained with the Maxey–Eakin method of recharge estimation (Maxey and Eakin, 1949).

Discharge from the WRFS occurs principally as spring discharge. Major spring discharge occurs in three areas: (1) White River Valley, where discharges of $\sim 0.861\,m^3\,s^{-1}$ of warm water ($> 20°C$) and $\sim 0.548\,m^3\,s^{-1}$ of cold water occur; (2) Pahranagat Valley, where a discharge of $\sim 0.978\,m^3\,s^{-1}$ of warm water occurs; (3) Muddy River Springs in Upper Moapa Valley, where a discharge of $\sim 1.408\,m^3\,s^{-1}$ of warm water occurs. Very little variation in discharge has been noted for these springs. Evaporation of discharge from Pahranagat Valley springs occurs principally from Pahranagat and Maynard Lakes.

Discharge of groundwater by evapotranspiration (ET) in valleys not associated with regional springs is $\sim 0.196\,m^3\,s^{-1}$ and occurs principally in Long ($0.086\,m^3\,s^{-1}$), Garden ($0.078\,m^3\,s^{-1}$), and Cave ($0.008\,m^3\,s^{-1}$) Valleys (Eakin, 1966). Evapotranspiration estimates are considered rough approximations. This study has adopted the ET estimates of Eakin as the more rigorous approach of phreatophyte mapping was beyond the scope of this study.

Winograd and Friedman (1972) postulated several changes to Eakin's conceptual model and questioned the validity of a water-budget-based model in light of environmental isotopic data in the region. They concluded that: (1) significant underflow from Pahranagat Valley via the Pahranagat Shear Zone exists; (2) discharge from Muddy River Springs may be derived from the Spring Mountains, west of Las Vegas, rather than the WRFS, despite the groundwater barrier effects of the Las Vegas Shear Zone; (3) the 13‰ difference between the observed deuterium value at Pahranagat Springs in Pahranagat Valley and Muddy River Springs is because of variation of deuterium recharge concentration with time.

Welch and Thomas (1984) proposed other modifications to Eakin's model of the system. Results of mass-balance calculations using deuterium isotope data and recharge and discharge estimates reveal greatly reduced flow past areas of major discharge in the White River and Pahranagat Valleys.

Other contributions to hydrologic data of the WRFS have been made by Eakin (1962, 1963a, b, 1964), Mifflin (1968), and Mifflin and Hess (1979). Potentiometric mapping of the region by Thomas et al. (1985) has resulted in the elimination of Long Valley from the flow system, assuming that hydraulic gradients in the alluvium are similar to those in the underlying carbonate aquifer.

DISCRETE-STATE COMPARTMENT MODEL

A discrete-state compartment (DSC) model (Simpson and Duckstein, 1976) was used to simulate flow in the WRFS. The DSC code was developed by Campana (1975) and applied to the Tucson Basin by Campana and Simpson (1984), and the Edwards aquifer by Campana and Mahin (1985).

Discrete-state compartment models are nothing more than sophisticated mixing-cell models, which represent the given hydrogeological system as a network of interconnected cells, through which water and dissolved materials are transported. A recursive form of the conservation of mass equation governs the transport of water and dissolved matter. For any given cell, the basic equation of the DSC model is (Simpson and Duckstein, 1976)

N is iteration step, not time step, since system in steady state

$$S(N) \;=\; S(N-1) + [\mathrm{BRV}(N) \times \mathrm{BRC}(N)] - [\mathrm{BDV}(N) \times \mathrm{BDC}(N)] \qquad (1)$$

where: $S(N)$ is the cell state at iteration N, the mass or amount of tracer in the cell; BRV(N) is the boundary recharge volume at iteration N, the input volume of water to the cell; BRC(N) is the boundary recharge concentration at iteration N, the input concentration of tracer; BDV(N) is the boundary discharge volume at iteration N, the output volume of water from the cell; BDC(N) is the boundary discharge concentration at iteration N, the output concentration of tracer.

The tracer concentration in the water, or in this case, the deuterium value of the recharge water, entering a boundary cell from outside the model's boundaries, is referred to as a system boundary recharge concentration (SBRC). The volume of recharge water entering a boundary cell is referred to as a system boundary recharge volume (SBRV).

Equation (1) is applied successively to each cell in the network during a given iteration. As a result, boundary discharge volumes and concentrations from 'upstream' cells become boundary recharge volumes and concentrations to 'downstream' cells. The BDC(N) term is the only unknown on the right side of eq. (1). Its value can be ascertained by specifying one of two mixing rules: the simple mixing cell (SMC) rule or the modified mixing cell (MMC) rule. The former rule simulates perfect mixing within a cell, and the latter imitates some middle ground between perfect mixing and pure piston flow. For the SMC

$$\mathrm{BDC}(N) \;=\; \{S(N-1) + [\mathrm{BRV}(N) \times \mathrm{BRC}(N)]\}/[\mathrm{VOL} + \mathrm{BRV}(N)] \qquad (2)$$

where VOL is the volume of water in the cell.

For the MMC

$$\mathrm{BDC}(N) \;=\; S(N-1)/\mathrm{VOL} \qquad (3)$$

The MMC approaches pure piston flow as the BRV approaches VOL, and approaches perfect mixing as the BRV approaches zero. This study used both options. As the model approached calibration, the model-derived deuterium values were almost identical for both SMC and MMC options.

Each cell in the DSC model depicts a region of the hydrogeological system; regions are differentiated based upon their hydrogeological uniformity and the availability of the data. Variability within the system is distributed between cells. Cells can be of any desired size and can be arranged in a one-, two-, or three-dimensional configuration.

Discrete-state compartment models permit the user to specify the flow paths between cells and the discharge from the system. To do so requires an initial estimate of the flow system, such that an initial set of specifications can be established. During the calibration process, these parameters are adjusted by the modeler to obtain agreement between the simulated and observed tracer concentrations.

DEUTERIUM AS A GROUNDWATER TRACER

The stable isotope deuterium (^{2}H or D) was chosen as the tracer in the DSC model. Deuterium is a useful groundwater tracer because it: (1) is part of the water molecule; (2) does not decay with time; (3) is not removed from water by exchange processes during movement through most aquifer materials; (4) experiences no hydrodynamic dispersion. The deuterium content of precipitation varies with latitude and elevation. Variations are caused principally by the history of isotopic fractionation that occurred during changes of state of water between vapor, liquid, and solid. These variations serve to 'fingerprint' water masses, which is reflected by the spatial distribution of deuterium in concentrations in groundwater.

The measurement of deuterium content is made with a mass spectrometer. As absolute quantities of stable isotopes are difficult to measure, the isotopes of hydrogen are measured as the ratio between the element's heavy and light isotopic species. The relative permil (‰, i.e. parts per thousand) deviation of the sample isotopic ratio from that of the standard is defined as

$$\delta D \;=\; 1000[(D/H)_{\mathrm{sample}} - (D/H)_{\mathrm{standard}}]/(D/H)_{\mathrm{standard}} \;=\; 1000(R_{\mathrm{D}} - 1) \qquad (4)$$

where R_{D} is the ratio between the heavy to light isotope ratio of the sample to that of the standard. A depletion of heavy isotopes in the sample, measured with respect to the standard, corresponds to a negative δD value. The abbreviation is usually understood to represent permil units. In this study, the standard is Vienna Standard Mean Ocean Water (V-SMOW).

In using deuterium as a groundwater tracer, the following assumptions are implicit: (1) recharge waters can be assigned a characteristic deuterium value; (2) the deuterium signature of recharge is a function of the geographic location (latitude, elevation, distance from the ocean, and temperature); (3) deuterium is a conservative tracer. With regard to the first two assumptions, deuterium samples from high-altitude springs were assumed to be representative of recharge waters from a given mountain range. The third assumption is critical to the successful use of deuterium as a groundwater tracer. This assumption can be invalid if fractionation or isotopic exchange has occurred subsequent to recharge. Although exchange of deuterium may occur in some hydrogen-bearing clays, it is not considered a significant process in this system.

The question of the time invariance of deuterium signatures of the recharge water and the recharge rate itself is a valid one. Paleoclimatically induced shifts in each quantity have no doubt occurred in the past. With the exception of preliminary work by Winograd et al. (1985), which dealt with waters older than the groundwaters in the WRFS, no quantitative investigations have been undertaken to determine these paleoclimatically induced shifts in eastern Nevada. Claassen (1983) interpreted the distribution of δD plotted against ^{14}C-derived ages as an indication of a deviation from the mean annual temperature. Mifflin and Wheat (1979) estimated, based on Pleistocene lake levels in the Great Basin, a mean annual temperature decrease of 5°C and a mean annual precipitation increase of ~68% during the lacustrine episodes. These studies suggest possible paleoclimatically induced shifts in both deuterium signatures and recharge rates. As quantitative shift data are lacking, the model described herein assumed time-invariation recharge rates and deuterium signatures.

Seventy-four deuterium values were used in this study, 34 of which were used for SBRC (recharge signature) determination and the remainder for calibration. Of the total, 25 samples were collected and analyzed by the Desert Research Institute (DRI). Eighteen of the DRI samples were collected in June 1986 as a part of this study. The remaining data were selected from the United States Geological Survey (USGS) data base in Reston, VA. The complete data suite can be found in Kirk and Campana (1988).

DEVELOPMENT OF THE WHITE RIVER FLOW SYSTEM DSC MODEL

Flow scenarios

Because of the dearth of data on the WRFS, the uncertainties in the information available (saturated thicknesses, recharge volumes, effective porosities, etc.) and the large number of degrees of freedom in the DSC model, three different flow scenarios were simulated. This approach leads to estimates of the range in a certain parameter (e.g. volume of storage in the carbonate aquifer) as opposed to a single value. Although a large number of flow scenarios could be specified, the three selected were designed to address the following aspects of the WRFS: (1) the differences in deuterium concentration between the Pahranagat Valley springs (average: −108‰) and the carbonate wells in Coyote Spring Valley (average: −101‰); (2) the differences in deuterium concentration between the carbonate wells of Coyote Spring Valley and Muddy River Springs (−98‰); (3) distribution of groundwater flow in the White River Valley; (4) existence of underflow from Long Valley into Jakes Valley. Each scenario consists of an overlying alluvial aquifer (tier 1) and an underlying carbonate aquifer (tier 2).

Scenario 1 divides the WRFS into 22 cells (Fig. 4), composed of two tiers. Alluvial (tier 1) and carbonate (tier 2) aquifers were specified for Jakes, White River, Cave, Coal/Garden, Dry Lake, and Delamar Valleys. Alluvial aquifers were not specified for Pahroc, Pahranagat, Coyote Spring, Kane Springs, Lower Meadow and Upper Moapa Valleys, because of the relatively small

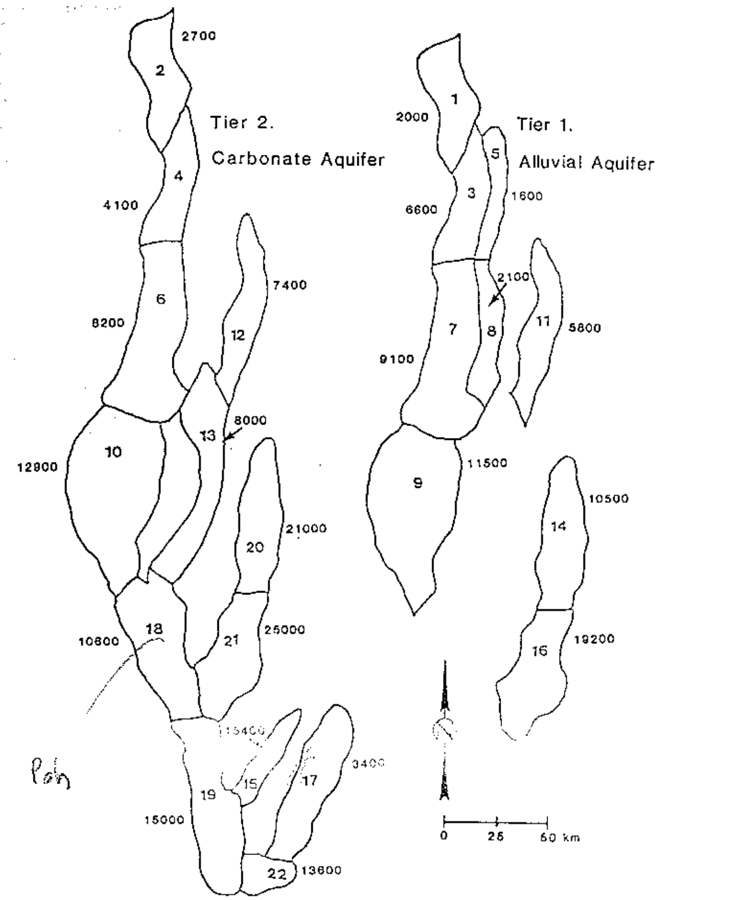

Fig. 4. Cell configuration for WRFS Scenario 1. Large numbers adjacent to cells are water mean ages (years).

volume of the alluvial aquifers compared with the carbonate aquifers in these basins and the lack of isotope data. Long Valley has been excluded and Lower Meadow Valley included in the WRFS based on potentiometric mapping by Thomas et al. (1985) and a reconnaissance report by Rush (1964). The areal extent of each cell coincided with exposed alluvium in each of the hydrographic basins, based upon available geological maps.

Scenario 2 divides the WRFS into 20 cells (Fig. 5). Preston Springs in

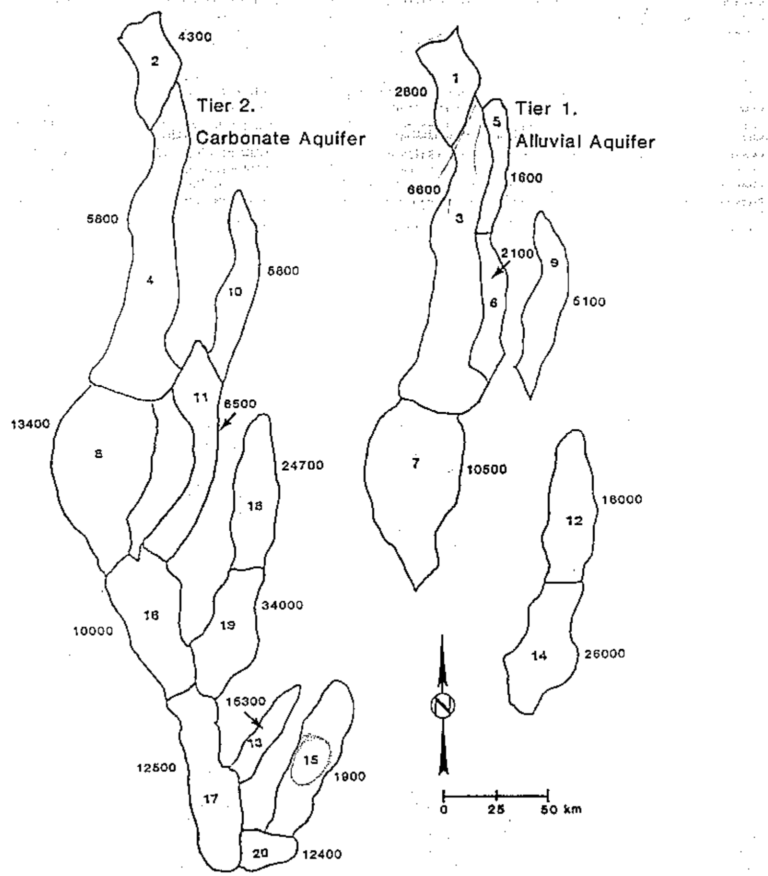

Fig. 5. Cell configuration for WRFS Scenario 2. Large numbers adjacent to cells are water mean ages (years).

northwestern White River Valley is included in carbonate Cell 2 (Jakes Valley) with the remainder of White River Valley composed of four cells, as opposed to six cells in scenario 1. In addition, Scenario 2 adopts different intercellular flow paths and SBRV and SBRC values.

Scenario 3 introduces underflow from the Long Valley carbonate aquifer into the carbonate aquifer of Jakes Valley (Fig. 6). The amount of underflow is

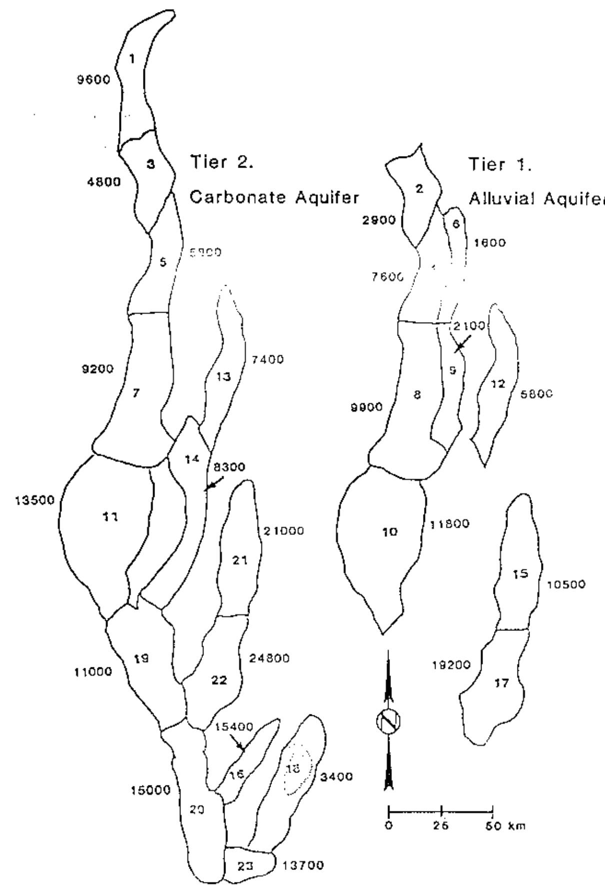

Fig. 6. Cell configuration for WRFS Scenario 3. Large numbers adjacent to cells are water mean ages (years).

small (20%) relative to the total volume of recharge estimated for Long Valley. Eakin's (1966) original model of the WRFS included Long Valley in the system. Although recent potentiometric mapping in the alluvial aquifer by Thomas et al. (1985) concluded that Long Valley is not part of the system, this does not preclude the possibility that the carbonate aquifer of Long Valley contributes to regional flow in the WRFS. Other than inclusion of Long Valley, scenario 3 is similar to scenario 1.

Cell volumes

Thicknesses of the Paleozoic carbonates exceed 9000 m locally in the WRFS. Estimates of the thicknesses of the carbonate and alluvial aquifers are difficult because of lack of deep borehole data, although some geophysical data were available. We assumed thicknesses of 3050 m for the carbonate cells and 610 m for the alluvial cells. Effective porosities for the carbonate and alluvial aquifers were assumed to be 3 and 15%, respectively. These cell volumes (area × thickness × porosity) for all scenarios are listed in Table 1; carbonate

TABLE 1

Cell volumes for Scenarios 1, 2 and 3

Cell no.	Scenario 1 ($10^9\ m^3$)	Scenario 2 ($10^9\ m^3$)	Scenario 3 ($10^9\ m^3$)
1	38.297	38.297	58.839*
2	38.297*	38.297*	38.297
3	63.931*	136.468	38.297*
4	63.931*	136.468*	63.931
5	19.198	19.198	63.931*
6	72.550*	24.044	19.198
7	72.550	107.912	72.550*
8	24.044	107.912*	72.550
9	107.912	49.937	24.044
10	107.912*	49.937*	107.912
11	49.937	52.452*	107.912*
12	49.937*	97.160	49.937
13	52.452*	18.865*	49.937*
14	97.160	47.421	52.452*
15	18.865*	18.865*	97.160
16	47.421	54.807*	18.865*
17	18.865*	66.261*	47.421
18	54.807*	97.160*	18.865*
19	66.261*	47.421*	54.807*
20	97.160*	0.543*	66.261*
21	47.421*		97.160*
22	0.543*		47.421*
23			0.543*
Totals	1209.451	1209.302	1268.288

* Carbonate cell.

cells are designated by an asterisk, a convention that will be used throughout this paper. We feel that these cell volumes are reasonable given the few data, and represent 'average' values. Should more detailed information become available, it can be easily incorporated into the model. It should be noted that the cell volume equals the volume of water in a given cell.

System boundary recharge volumes

The SBRV estimate for each boundary cell was based initially on recharge estimates calculated by the Maxey–Eakin method of recharge estimation. Table 2 shows the calibrated SBRV for each cell used in the three scenarios; Table 3 shows the recharge estimates on a hydrographic basin basis for each scenario and the corresponding estimate from Eakin (1966). The amount of recharge assigned to the carbonate cells is speculative, as virtually no quantitative estimates of mountain block recharge have been reported in the literature.

System boundary recharge concentrations

Each SBRV in the model is assigned a characteristic isotopic signature or system boundary recharge concentration. Table 4 shows the estimated SBRC

TABLE 2

Calibrated system boundary recharge volumes for Scenarios 1, 2 and 3

Cell no.	Scenario 1 ($m^3 s^{-1}$)	Scenario 2 ($m^3 s^{-1}$)	Scenario 3 ($m^3 s^{-1}$)
1	0.626	0.430	0.196*
2	0.274*	0.391*	0.430
3	0.196	0.235	0.274*
4	0.196*	0.430*	0.196
5	0.391	0.391	0.196*
6	0.156*	0.313	0.391
7	0.117	0.274	0.156*
8	0.313	0.156*	0.117
9	0.274	0.313	0.313
10	0.156*	0.235*	0.274
11	0.274	0.078*	0.156*
12	0.156*	0.196	0.274
13	0.078*	0.039*	0.156*
14	0.293	0.059	0.078*
15	0.039*	0.313*	0.293
16	0.078	0.059*	0.039*
17	0.176*	0.235*	0.078
18	0.059*	—	0.176*
19	0.196*	—	0.059*
20	—	—	0.196*

* Carbonate cell.

TABLE 3

Recharge to WRFS hydrographic basins

Hydrographic basin	Eakin (1966) ($m^3 s^{-1}$)	Scenario 1 ($m^3 s^{-1}$)	Scenario 2 ($m^3 s^{-1}$)	Scenario 3 ($m^3 s^{-1}$)
Long Valley	0.391	—	—	0.196
Jakes Valley	0.665	0.900	0.822	0.704
White River Valley	1.448	1.369	1.369	1.369
Coal/Garden Valleys	0.391	0.430	0.430	0.430
Cave Valley	0.548	0.430	0.548	0.430
Pahroc Valley	0.086	0.078	0.078	0.078
Dry Lake Valley	0.196	0.293	0.196	0.293
Kane Springs Valley	—	0.039	0.039	0.039
Delamar Valley	0.039	0.078	0.059	0.078
Pahranagat Valley	0.078	0.059	0.059	0.059
Coyote Spring Valley	0.102	0.196	0.235	0.196
Lower Meadow Valley	0.313*	0.176	0.313	0.176
Totals	4.257	4.049	4.147	4.049

*From Rush (1964).

TABLE 4

System boundary recharge concentrations

Cell	Scenario 1 (‰ δD)	Scenario 2 (‰ δD)	Scenario 3 (‰ δD)
1	−124.0	−124.0	−126.0*
2	−124.0*	−124.0*	−124.0
3	−113.0	−112.0	−124.0*
4	−113.0*	−112.0*	−113.0
5	−113.0	−113.0	−113.0*
6	−110.5*	−104.0	−113.0
7	−110.5	−104.0	−110.5*
8	−104.0	−104.0*	−110.5
9	−103.0	−102.0	−104.0
10	−103.0*	−102.0*	−103.0
11	−102.0	−100.0*	−103.0*
12	−102.0*	−97.0	−102.0
13	−100.0*	−87.0*	−97.0*
14	−96.0	−87.0	−100.0*
15	−87.0*	−89.0*	−97.0
16	−87.0	−89.0*	−87.0*
17	−89.0*	−93.0*	−87.0
18	−89.0*	—	−89.0*
19	−93.0*	—	−89.0*
20	—	—	−93.0*

*Carbonate cell.

inputs for all cells in the three scenarios. The SBRC for each cell receiving recharge was based on deuterium samples from high-altitude springs. We assumed that averaging deuterium values from high-altitude springs of a given mountain range yielded an average deuterium signature of recharge waters. In the case of Lower Meadow Valley, an average deuterium value based upon isotope data from wells in the valley was used for the SBRC. The average value (−89.0‰ δD) was assumed to represent the isotopic signature of underflow from Lower Meadow Valley into Upper Moapa Valley.

Flow distributions

During calibration, flow distributions among cells were adjusted to obtain agreement with observed δD values. Intercellular flow paths are shown in Figs. 7–9.

We assumed that virtually all groundwater in the alluvial aquifer flows into the underlying carbonate aquifer in Jakes, Cave, Coal/Garden, Dry Lake, and Delamar Valleys. Scenario 1 assumes downward flow in the southern portion of the White River Valley, whereas Scenario 2 assumes a net upward flow from the carbonates to the alluvium. These assumptions depend on whether we divide the western half of White River Valley into four cells (Scenario 1) or two cells (Scenario 2).

System boundary discharge volumes

System boundary discharge volumes (SBDV) in the form of springflow, ET, or underflow out of the system for Scenarios 1, 2 and 3 are listed in Table 5. Underflow out of the system, which is determined by calibration, is included in the SBDV. Underflow out of the system occurs only in Pahranagat and Upper Moapa Valleys. Springflow from the carbonate aquifers is relatively constant. The system is in steady state, i.e. total recharge = total discharge.

Eakin (1966) estimated 0.078 $m^3 s^{-1}$ of ET in Garden Valley (Cell 9, Scenario 1) and assumed that in valleys where regional springs discharge, nearly all discharged water is subsequently consumed by ET; Eakin considered ET to be minor in all other valleys. This assumption may be in error, but is adopted for this regional analysis. In lieu of phreatophyte mapping in the study area, Eakin's (1966) estimates were used. Discharge from the system because of pumping was not considered, owing to the relatively short duration of pumping (40 years) compared with the age of the water in the flow system.

RESULTS AND DISCUSSION

Calibration

Calibration was accomplished by trial and error. The intercellular flow distributions and recharge rates were adjusted to achieve calibration, with the

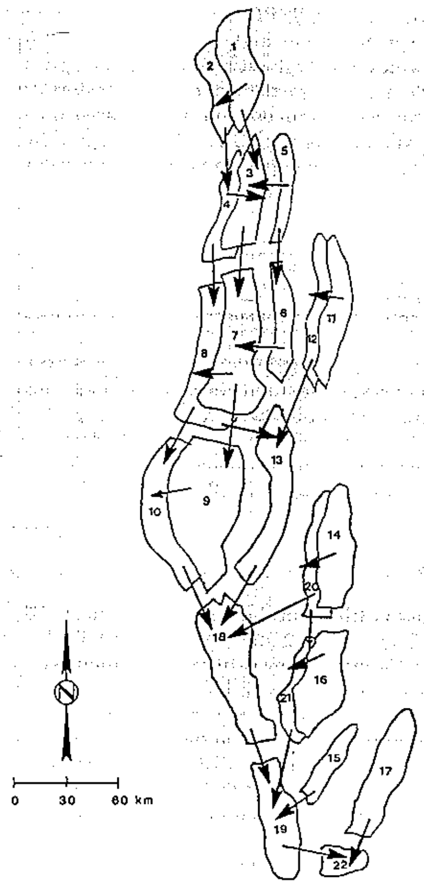

Fig. 7. Flow distributions for WRFS Scenario 1.

former subject to more adjustment than the latter. The model was run until calculated deuterium values did not change to the first decimal place. Both the real-world system and its model representation are assumed to be in steady state with respect to deuterium values. Calibration was achieved when the model-derived deuterium value agreed to within 2‰ with the observed deuterium value which had been assigned to a given cell. In some instances there was a trade-off and calibration within 2.5‰ was the best fit attained.

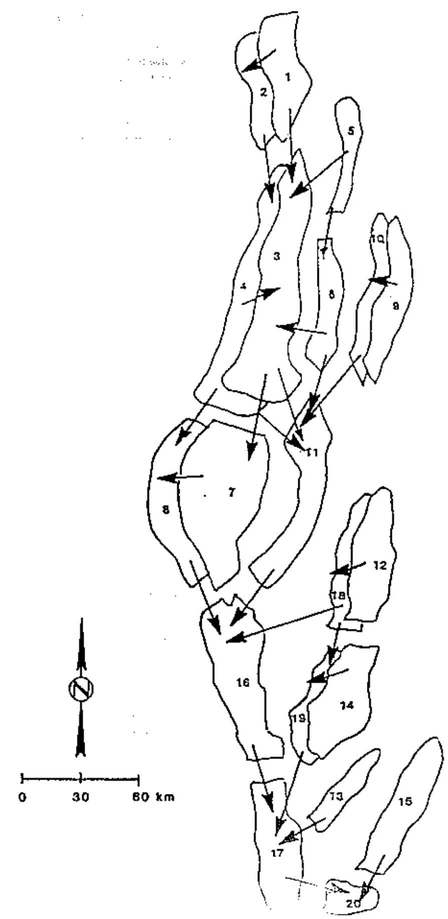

Fig. 8. Flow distributions for WRFS Scenario 2.

Calibration results were previously given in Tables 2 (SBRV or recharge rates to the model boundaries), 3 (recharge rates to hydrographic basins) and 5 (SBDV or discharge rates across the model boundaries). Table 6 shows the observed and calculated deuterium values, and Tables 7 and 8 show parameter ranges for the carbonate and alluvial systems, respectively.

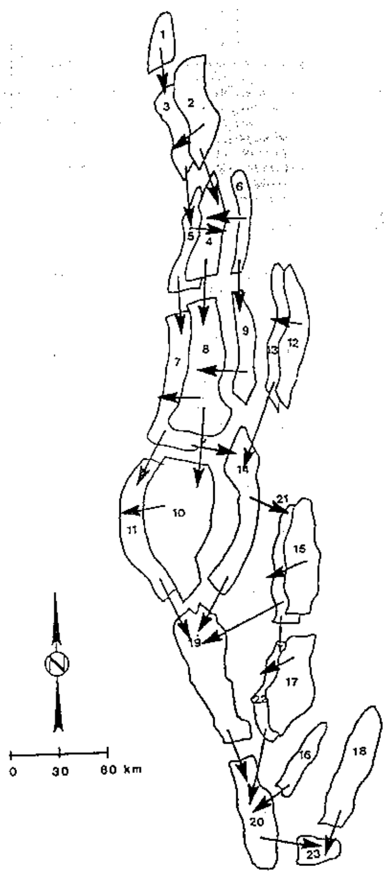

Fig. 9. Flow distributions for WRFS Scenario 3.

Differences among Scenarios 1, 2 and 3

Scenario 1 was calibrated by: (1) diverting $0.172\,m^3\,s^{-1}$ from the system (west from Cell 18*) along the Pahranagat Shear Zone; (2) specifying $0.196\,m^3\,s^{-1}$ of recharge from the Sheep Range to Coyote Spring Valley (Cell 19*); (3) including $0.176\,m^3\,s^{-1}$ of underflow from Lower Meadow Valley (Cell 17*) into Upper Moapa Valley (Cell 22*); (4) increasing recharge to Dry Lake Valley to $0.293\,m^3\,s^{-1}$, 50% more than the Maxey–Eakin estimate; (5) increasing the recharge to Delamar Valley from 0.039 to $0.078\,m^3\,s^{-1}$; (6) allowing most ($0.345\,m^3\,s^{-1}$) of the combined groundwater flow from Dry Lake and Delamar Valleys to discharge at Coyote Spring (Cell 19*).

The following were required to calibrate Scenario 2: (1) dividing the western half of White River Valley into two cells, 3 and 4*, with upward vertical hydraulic gradients from Cell 4* to Cell 3; (2) allowing discharge from alluvial Cell 3 to the carbonate cell of Pahroc Valley (13*); (3) specifying that underflow from Cell 4* to Cell 8* of Coal/Garden Valleys is ~24% of the corresponding flow distribution in Scenario 1 (0.047 and $0.192\,m^3\,s^{-1}$, respectively); (4) discharging $0.145\,m^3\,s^{-1}$ from the system along the Pahranagat Shear Zone; (5) permitting groundwater flow of $0.188\,m^3\,s^{-1}$ from Delamar Valley to Coyote Spring Valley (as opposed to the $0.345\,m^3\,s^{-1}$ adopted in Scenario 1); (6) specifying $0.235\,m^3\,s^{-1}$ of recharge from the Sheep Range to Coyote Spring Valley (Cell 17*); (7) allowing $0.313\,m^3\,s^{-1}$ of groundwater to flow from Lower Meadow Valley (Cell 15*) into Upper Moapa Valley (Cell 20*); (8) diverting $\sim 0.117\,m^3\,s^{-1}$ from the system as underflow from Upper Moapa Valley into Moapa Valley. Scenario 2 represents the maximum amounts of recharge from the Sheep Range and underflow from Lower Meadow Valley.

Scenario 3 used the calibrated inputs of Scenario 1, together with the introduction of $0.196\,m^3\,s^{-1}$ of underflow from Long Valley (Cell 1*) and a corresponding decrease in recharge assigned to Jakes Valley (Cell 3*). Calibration was achieved by decreasing the SBRC of Cell 15 (Dry Lake Valley) by 2‰ and permitting flow from Cell 7* (White River Valley) to Cell 14* (Pahroc Valley).

Despite the differences among the scenarios, certain similarities exist.

TABLE 5

Calibrated system boundary discharge volumes

Cell no.	Scenario 1 ($m^3\,s^{-1}$)	Scenario 2 ($m^3\,s^{-1}$)	Scenario 3 ($m^3\,s^{-1}$)
4	0.446*	0.863*	—
5	0.200	0.198	0.448*
6	0.436*	0.335	0.200
7	—	0.052	0.437*
8	0.340	—	—
9	0.077	—	0.340
10	—	—	0.077
16	—	1.065*	—
18	1.148*	—	—
19	—	—	1.131*
20	—	1.634*	—
22	1.401*	—	—
23	—	—	1.420*

* Carbonate cell.

TABLE 6

Observed and calculated deuterium values

Cell no.	Scenario 1			Scenario 2			Scenario 3		
	Observed (‰ δD)	Calculated (‰ δD)	Difference (‰ δD)	Observed (‰ δD)	Calculated (‰ δD)	Difference (‰ δD)	Observed (‰ δD)	Calculated (‰ δD)	Difference (‰ δD)
1		−124.0			−124.0			−126.0	
2		−124.0			−124.0			−124.0	
3	−119.0	−118.3	0.7	−119.0	−116.8	2.2		−124.4	
4	−124.5	−122.0	2.5	−120.0	−119.6	0.4	−119.0	−118.5	0.5
5	−113.0	−113.0	0.0	−113.0	−113.6	0.6	−124.5	−122.4	2.1
6	−119.0	−117.7	1.3	−106.0	−107.9	−1.9	−113.0	−113.0	0.0
7	−118.3	−116.7	1.6	−107.5	−109.0	−1.5	−119.0	−117.8	1.2
8	−106.0	−107.4	−1.4	−110.0	−108.6	1.4	−118.3	−116.8	1.5
9	−107.5	−107.0	0.5	−100.0	−102.0	−2.0	−106.0	−107.4	−1.4
10	−110.0	−109.2	0.8		−102.0		−107.0	−107.1	−0.1
11	−100.0	−102.0	−2.0	−108.0	−107.0	1.0	−110.0	−109.3	−0.7
12		−102.0		−95.0	−97.1	−2.1	−100.0	−102.0	−2.0
13	−108.0	−107.6	0.4	−88.0	−87.0	1.0		−102.0	
14	−95.0	−96.0	−1.0	−88.0	−88.8	−0.8	−108.0	−107.7	0.7
15		−87.1			−89.0		−95.0	−97.0	−2.0
16	−87.0	−87.6	−0.6	−108.0	−106.5	1.5		−87.0	
17		−89.0		−100.5	−101.8	−1.3	−87.0	−87.2	−0.2
18	−108.0	−107.4	0.6		−97.1			−89.0	
19	−100.5	−100.8	−0.3		−95.3		−108.0	−107.5	0.5
20		−97.0		−98.0	−98.8	−0.8	−100.5	−100.9	0.4
21		−95.1						−97.0	
22	−98.0	−99.3	−1.3					−95.0	
23							−98.0	−99.4	−1.4

Difference = calculated − observed.

TABLE 7

Parameter ranges for the carbonate system

Parameter	Scenario 1	Scenario 2	Scenario 3
Recharge rates ($m^3 s^{-1}$)	1.487	1.937	1.682
Storage volumes ($10^9 m^3$)	690.5	690.5	752.1
Mean ages (years)	2700–25 000	4300–34 000	4800–24 800

TABLE 8

Parameter ranges for the alluvial system

Parameter	Scenario 1	Scenario 2	Scenario 3
Recharge rates ($m^3 s^{-1}$)	2.563	2.210	2.367
Storage volumes ($10^9 m^3$)	517.9	517.9	517.9
Mean ages (years)	1600–19 200	1600–26 000	1600–19 200

Regardless of the scenario, calibration required: (1) the diversion of ground water outside the WRFS from Pahranagat Valley; (2) an increase in recharge from the Sheep Range; (3) the introduction of underflow from Lower Meadow Valley into Upper Moapa Valley. The greatly increased recharge from the Sheep Range, just west of Coyote Spring Valley, is supported by a water budget of Las Vegas Valley by Harrill (1979), who estimated that 0.078 $m^3 s^{-1}$ of recharge from the Sheep Range flows to Las Vegas Valley, leaving the remaining estimated 0.364 $m^3 s^{-1}$ of recharge available to Coyote Spring Valley and Desert Valley, which is just west of the Sheep Range. The attribution of underflow from Lower Meadow Valley into Upper Moapa Valley is based upon reconnaissance work by Rush (1964), who estimated that 0.313 $m^3 s^{-1}$ is discharged from Lower Meadow Valley as underflow. Finally, it is feasible that a certain percentage of ground water entering Upper Moapa Valley is not discharged at Muddy River Springs but subsequently flows into Moapa Valley.

Recharge rates

System boundary recharge volumes (recharge rates) on a cell-by-cell basis were given in Table 2. Table 3 listed recharge rates on a valley-by-valley (hydrographic basin) basis and Tables 7 and 8 summarized recharge rates to the carbonate and alluvial aquifers, respectively.

The data in Table 3 indicate that whereas the valley-by-valley recharge rates may differ greatly, the total recharge rates are virtually the same. This holds regardless of whether comparisons are made among the various DSC model scenarios or between the DSC model estimates and the water-budget approaches of Eakin (1966) and Rush (1964). Among the scenarios, significant differences can be found in Dry Lake and Lower Meadow Valleys. Scenarios 1 and 3, virtually identical except for the inclusion of Long Valley in Scenario 3, yield identical recharge rates to the aforementioned valleys; the Scenario 2 recharge rate is 33% lower in Dry Lake Valley and ~78% greater in Lower Meadow Valley. When compared with the water-budget figures, the DSC model estimates are > 90% greater in Coyote Spring Valley; this increase is the result of increased recharge from the Sheep Range. Scenario 1 and 3 recharge estimates for Lower Meadow Valley are also significantly lower than either the Rush (1964) or the Scenario 2 estimate, which were identical.

from Eakin (1966)

geologically then works

Unlike the water-budget approach of Eakin and Rush, the DSC model is capable of distinguishing between recharge to the alluvial system and that to the carbonate system. The disadvantage to this is that, given the current state of knowledge, it is virtually impossible to verify these numbers, especially carbonate system recharge. However, these estimates should be viewed as first approximations, which can serve as starting points for more sophisticated models or planning purposes.

Pahranagat Shear Zone underflow

Eakin's (1966) original conceptual model of the WRFS did not allow for subsurface flow outside the flow system boundaries. However, to achieve calibration, each scenario required the diversion of flow west from Pahranagat Valley along the Pahranagat Shear Zone. Scenarios 1 and 3 diverted $0.172\ m^3 s^{-1}$ in this manner, whereas Scenario 2 diverted $0.145\ m^3 s^{-1}$ along this zone. Winograd and Friedman (1972) hypothesized that ~35% of the discharge at Ash Meadows, or ~$0.235\ m^3 s^{-1}$, originated in Pahranagat Valley. Ash Meadows is a groundwater discharge area outside the WRFS located near the Nevada–California border ~160 km west of the WRFS terminus. It is the major discharge area for another regional carbonate flow system underlying and extending beyond the Nevada Test Site. Although the DSC underflow estimates are lower than that of Winograd and Friedman, they nevertheless provide additional evidence that the WRFS is not completely closed in the subsurface and is undoubtedly linked to at least one other regional carbonate flow system.

Storage estimates

The cell volume is the volume of water contained within the boundaries of that cell. Individual cell volumes were shown in Table 1, and estimates of the total amount of water in storage can be obtained by simply summing cell volumes. Tables 1, 7 and 8 showed these totals. The water storage figures for the carbonate system are the only known estimates for the WRFS and cannot be verified at this juncture. However, they do represent starting points for water resource planners who, before this, had little notion of the amount of water stored in the carbonate portion of the White River system.

Mean ages and age distributions

One of the advantages of using DSC models with tracer data is that once calibrated, the models will yield the mean ages of the water in the various regions (cells) of the system. This feature allows us to obtain water ages using stable tracers. Mean ages for Scenarios 1, 2 and 3 were previously shown in Figs. 4, 5, and 6, respectively; mean age ranges were given in Tables 7 and 8.

The groundwater mean ages shown in Figs. 4, 5 and 6 and Tables 7 and 8 are more useful than the decay ages that we might obtain from an environmental radioisotope such as ^{14}C, but they provide incomplete information in that nothing is learned about the median ages or the age distributions from which the means are derived. Some knowledge of the median ages, which are not necessarily equal to the corresponding mean ages, and the entire distribution of ages would be preferable to information on the mean ages alone. The entire age distribution could provide information on mixing and some indication of the age of the 'oldest' waters in a particular cell or aquifer region. Fortunately, DSC models can be used to produce age distributions and cumulative age distributions (Campana, 1987), so that we do not have to rely upon mean or median ages alone. If we had to rely on a single 'age', the median age is arguably more appropriate than the mean age, as, by definition, half the water in a given region is older than the median and half is younger. The mean age alone cannot provide such a breakdown.

As an illustrative example, the DSC cumulative age distribution function $F(N)$ was calculated for selected cells of Scenario 1. Three carbonate cells (2*, 10*, and 21*, representing Jakes, Coal/Garden, and Delamar Valleys, respectively) and three alluvial cells (1, 7, and 16, representing Jakes, a portion of White River, and Delamar Valleys, respectively) were selected as they represent cells in the upper (1 and 2*), middle (7 and 10*), and lower portions (16 and 21*) of the WRFS. Figures 10–15 show the cumulative age distribution function $F(N)$ for each cell. The mean age and median age, the age of the water at $F(N) = 0.5$, are shown on each graph. The striking differences between the mean and median ages are readily apparent. Groundwaters in excess of 100 000 years old are indicated in some of the regions, mainly the alluvial (Cell 16) and carbonate aquifers (Cell 21*) beneath Delamar Valley. Even in Cell 10*, the carbonate aquifer beneath Coal/Garden Valleys, the oldest ground water approaches 100 000 years old, although a higher percentage of the Delamar Valley ground waters are older than 100 000 years old. Jakes Valley (Cells 1 and 2*), at the very top of the flow system, naturally possesses the youngest waters, although a small percentage of the waters approach 15 000 years old in each cell. This detailed age information could not have been obtained from the mean or the median, either alone or together.

The shape of the $F(N)$ curve gives a qualitative indication of mixing in a

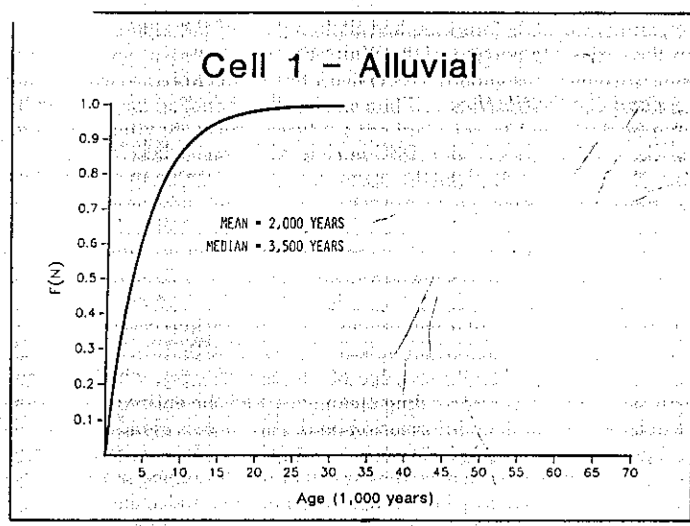

Fig. 10. Cumulative age distribution for Cell 1, Scenario 1.

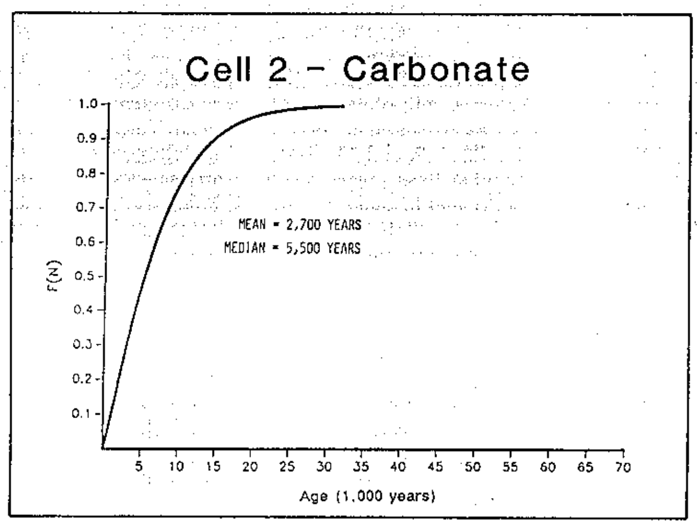

Fig. 11. Cumulative age distribution for Cell 2, Scenario 1.

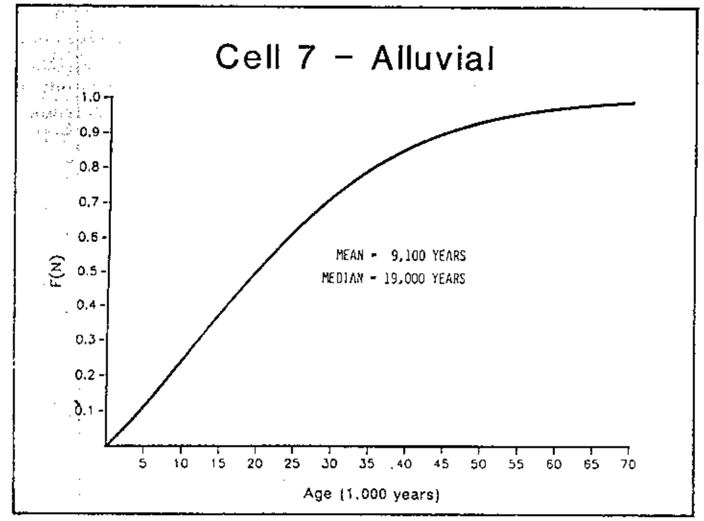

Fig. 12. Cumulative age distribution for Cell 7, Scenario 1.

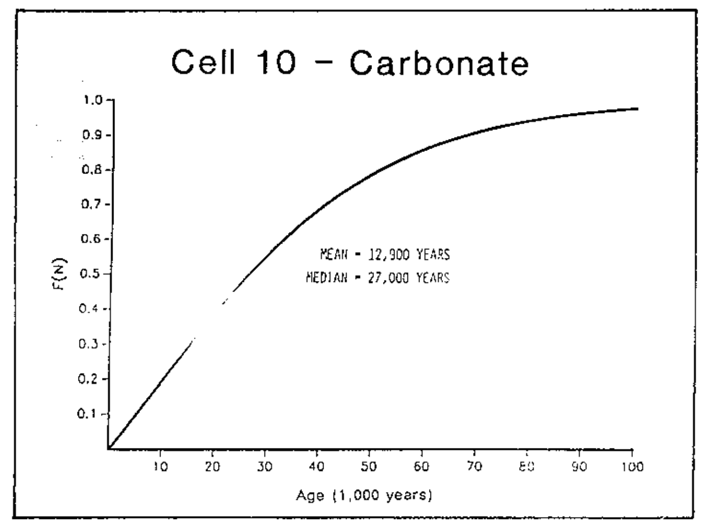

Fig. 13. Cumulative age distribution for Cell 10, Scenario 1.

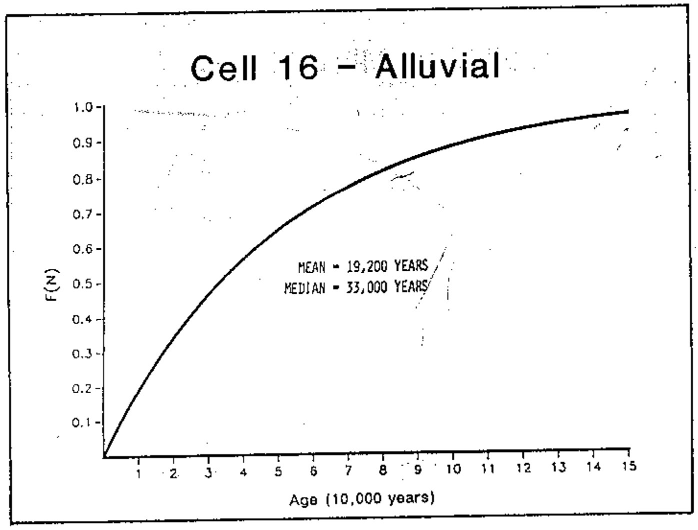

Fig. 14. Cumulative age distribution for Cell 16, Scenario 1.

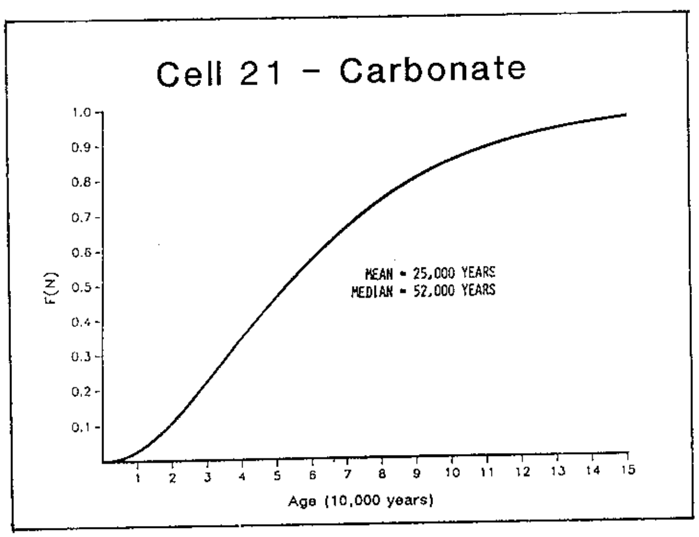

Fig. 15. Cumulative age distribution for Cell 21, Scenario 1.

given cell. A curve with a greater 'spread' about the median age indicates a higher degree of mixing than does one without as much 'spread'. The ground waters of Jakes Valley, at the top of the flow system, are the least well-mixed of the examples given, as they have had no opportunity to mix with other waters. As we move down the system, the ground waters in a given cell become better mixed as waters from different sources and of diverse ages commingle.

The ages alluded to above do not indicate the 'age' of the system; when we determine that a few per cent of the ground water beneath Delamar Valley are > 100 000 years old, we simply mean that this percentage of the water was recharged ~ 100 000 years ago. The flow system may have been 'operating' for millions of years. These age calculations, determined under steady conditions, might lead one to assume that the system has been in a steady-state mode for 100 000 years or so, an assumption that is very probably untrue. Climatic changes have occurred in the past 100 000 years in eastern Nevada, no doubt affecting recharge rates areas and effecting storage changes in the ground-water reservoir – changes that have not been considered [illegible]. Although the DSC model age distribution functions are not well defined for transient conditions, we can nevertheless attempt to construct a model of the WRFS, using transient inputs in an attempt to see if we can discern what recharge rates existed tens of thousands of years ago. Such attempts are now being considered.

CONCLUSIONS

Three DSC models, each addressing slightly different conceptual models of the WRFS, were constructed and calibrated. Although differences exist among the three scenarios, their gross characteristics are similar. The major inconsistency is Long Valley and whether or not it belongs in the flow system. The model can be calibrated with it (Scenario 3) or without it (Scenarios 1 and 2), so the Long Valley dilemma is unresolved. Certain consistencies exist, and an examination of these results in the following conclusions:

(1) with the exception of the White River Valley itself, flow is generally downward from the alluvial aquifer to the underlying carbonate aquifer;

(2) underflow with an average value of 0.163 $m^3 s^{-1}$ flows west from the Pahranagat Valley along the Pahranagat Shear Zone;

(3) Lower Meadow Valley is part of the WRFS and contributes underflow to Upper Moapa Valley;

(4) recharge from the Sheep Range to Coyote Spring Valley is at least 90% greater than that specified by Eakin (1966);

(5) recharge to the alluvial system is greater than that to the carbonate system;

(6) more water is stored in the carbonate system ($690.5 \times 10^9 m^3$–$752.1 \times 10^9 m^3$) than in the alluvial system ($517.9 \times 10^9 m^3$);

(7) groundwater mean ages range from 1600 to 26 000 years in the alluvial system and from 2700 to 34 000 years in the carbonate system;

(8) the oldest ground waters in each system are older than 100 000 years;
(9) the stable isotope deuterium can be used to calibrate simple groundwater flow models and provide groundwater ages;
(10) DSC models are capable of providing more detailed groundwater age information (means, medians and the entire age distribution) than other models.

Drawbacks do exist. For example, as none of the scenarios account for transience in either recharge rates or their deuterium signatures, these quantities represent long-term averages. Both long-term and short-term variations in each of these quantities have occurred. The effects of these variations on model calibration and results are now under investigation. Another questionable aspect involves the use of high-elevation springs to determine the deuterium signatures of recharge. Ideally, these signatures should be determined with time series data on deuterium but expense and site access difficulty precluded this. The problem of recharge deuterium signatures may be surmounted by sampling trees at suspected high-elevation recharge sites.

Despite the uncertainties inherent in a model of this type, the DSC model does provide first approximations to information that would be difficult or impossible to obtain otherwise. Some caution must be exercised in using this information, because as for other numerical models, the answers are non-unique. Discrete-state compartment models are perhaps more unconstrained than are other numerical models, so even greater caution must be exercised in using DSC model results. However, their greatest use perhaps lies in their application to sparse-data systems and their ability to test a number of different hypotheses, provide ranges in parameter estimates, guide the collection of additional data and serve as precursors for the development of more sophisticated models.

ACKNOWLEDGEMENTS

A number of individuals and organizations contributed to this research effort and deserve the authors' thanks. The State of Nevada, through its Carbonate Aquifer Studies Program, provided most of the funding. Additional support was provided by the Water Resources Center, Desert Research Institute. The senior author wishes to thank Marcia Olson Kirk for her advice, encouragement and patience. Deborah Wilson, Barbara Nauroth and Jan W[illegible] instrumental in producing this manuscript and Karla Cosens adroitly supervised its production. John W. Hess, Brad F. Lyles and W. Alan McKay unselfishly contributed their time to review the authors' efforts. The junior author wishes to thank Shirley Dreiss and James Gill of the Earth Sciences Board, University of California, Santa Cruz, for their hospitality during his sabbatical leave from the Desert Research Institute, when much of this paper was written. Finally, both authors extend a heartfelt thanks to John W. Hess, who served as Project Manager of the Institute's portion of the carbonate program.

REFERENCES

Campana, M.E., 1975. Finite-state models of transport phenomena in hydrologic systems. Ph.D. Dissertation, University of Arizona, Tucson, AZ, 252 pp. (unpublished).

Campana, M.E., 1987. Generation of ground-water age distributions. Ground Water, 25(1): 51–58.

Campana, M.E. and Mahin, D.A., 1985. Model-derived estimates of groundwater mean ages, recharge rates, effective porosities and storage in a limestone aquifer. J. Hydrol., 76: 247–264.

Campana, M.E. and Simpson, E.S., 1984. Groundwater residence times and recharge rates using a discrete-state compartment model and C-14 ages. J. Hydrol., 72: 171–185.

Claassen, H.C., 1983. Sources and mechanisms for ground-water recharge in the west-central Amargosa Desert, Nevada—a geochemical interpretation. U.S. Geol. Surv. Open-File Rep., 83–542, 58 pp.

Eakin, T.E., 1962. Ground water appraisal of Cave Valley in Lincoln and White Pine Counties, Nevada. Nevada Department of Conservation and Natural Resources, Ground Water Resource Reconnaissance Series, Rep. 13: 57 pp.

Eakin, T.E., 1963a. Ground water appraisal of Dry Lake and Delamar Valleys in Lincoln County, Nevada. Nevada Department of Conservation and Natural Resources, Ground Water Resource Reconnaissance Series, Rep. 16: 51 pp.

Eakin, T.E., 1963b. Ground water appraisal of Pahranagat and Pahroc Valleys in Lincoln and Nye Counties, Nevada. Nevada Department of Conservation and Natural Resources, Ground Water Resource Reconnaissance Series, Rep. 21: 37 pp.

Eakin, T.E., 1964. Ground water appraisal of Coyote Spring and Kane Springs Valleys, Lincoln and Clark Counties, Nevada. Nevada Department of Conservation and Natural Resources, Ground Water Resource Reconnaissance Series, Rep. 25: 61 pp.

Eakin, T.E., 1966. A regional interbasin groundwater system in the White River area, southeastern Nevada. Water Resour. Res., 2: 251–271.

Harrill, J.R., 1979. Pumping and ground water storage depletion in Las Vegas Valley, Nevada. U.S. Geol. Surv. Open-File Rep. 79-443: 76 pp.

Hess, J.W. and Mifflin, M.D., 1978. A feasibility study of water production from deep carbonate aquifers in Nevada. Desert Research Institute Tech. Rep., 41054: 125 pp.

Kellog, H.E., 1963. Paleozoic stratigraphy of the southern Egan Range, Nevada. Bull. Geol. Soc. Am., 74(6): 685–708.

Kirk, S.T. and Campana, M.E., 1988. Simulation of groundwater flow in a regional carbonate–alluvial system with sparse data: the White River flow system, southeastern Nevada. Desert Research Institue Tech. Rep., 41115: 76 pp.

Maxey, G.B. and Eakin, T.E., 1949. Ground water in the White River Valley, White Pine, Nye, and Lincoln Counties, Nevada. Nevada Department of Conservation and Natural Resources, Water Resour. Bull., 8: 54 pp.

McBeth, P.E., 1986. Hydrologic significance of Landsat Thematic Mapper lineament analysis in the Great Basin. M.S. Thesis, University of Nevada, Reno, NV, 154 pp. (unpublished).

Mifflin, M.D., 1968. Delineation of ground-water flow systems in Nevada. Desert Research Institute Tech. Rep., H-W 4: 54 pp.

Mifflin, M.D. and Hess, J.W., 1979. Regional carbonate flow systems in Nevada. J. Hydrol., 43: 217–237.

Mifflin, M.D. and Wheat, M.M., 1979. Pluvial lakes and estimated pluvial climates of Nevada. Nevada Bur. Mines Geol. Bull., 94: 42 pp.

Rush, F.E., 1964. Ground water appraisal of Meadow Valley Wash Area, Lincoln and Clark Counties, Nevada. Nevada Department of Conservation and Natural Resources, Ground Water Resource Reconnaissance Series, Rep., 27: 49 pp.

Simpson, E.S. and Duckstein, L., 1976. Finite state mixing-cell models. In: V. Yevjevich (Editor), Karst Hydrology and Water Resources. Vol. 2. Water Resource Publications, Ft. Collins, CO, pp. 489–508.

Stewart, J.H., 1980. Geology of Nevada. Nevada Bur. Mines Geol. Spec. Publ., 4: 136 pp.

Thomas, J.M., Mason, J.L. and Crabtree, J.D., 1985. Ground water levels in the Basin and Range. U.S. Geol. Surv. Hydrologic Atlas, HA-1a: 3 pp.
Tschanz, C.M. and Pampeyan, E.H., 1970. Geology and mineral deposits of Lincoln County, Nevada. Nevada Bur. Mines and Geol. Bull., 73, 187 pp.
Welch, A. and Thomas, J.M., 1984. Aqueous geochemistry and isotope hydrology of the White River System, eastern Nevada. Geol. Soc. Am. Abstr. Prog., 16(6): 689.
Winograd, I.J. and Friedman, I., 1972. Deuterium as a tracer of regional ground water flow, southern Great Basin, Nevada and California. Bull. Geol. Soc. Am., 83: 3691-3708.
Winograd, I.J., Szabo, B.J., Coplen, T.B., Riggs, A.C. and Kolesar, P.T., 1985. Two million year record of deuterium depletion in Great Basin groundwaters. Science, 227: 519-522.

Journal of Hydrology, 119 (1990) 389-391
Elsevier Science Publishers B.V., Amsterdam — Printed in The Netherlands

[4]

Short note

RELIABILITY BASED TIME AXES FOR FLOOD DATA PRESENTATION

W.E. BARDSLEY

Department of Earth Sciences, University of Waikato, Hamilton (New Zealand)

(Received and accepted for publication November 15, 1989)

It is standard for a major structure in a river environment to have some predetermined N-year operational lifetime. The design requirement is then to build in such a way that there is a sufficiently high probability R that the largest flood event in N years will not cause major damage or destruction. The probability R here represents the reliability of the structure with respect to its intended lifetime (Mays, 1987, p. 229).

It is well known that designing against the N-year return period magnitude is not consistent with a high reliability for an N-year lifetime. Specifically, designing against the N-year event will generate a reliability not exceeding $R = 0.37$ (assuming stationarity). Design magnitudes are therefore usually set so that the return period concerned is considerably longer than the intended operational lifetime of the structure.

Apart from the obvious practical problem of extrapolation, the use of long return periods in design work raises questions with respect to both validity and perception. First, it is questionable to speak of designing against (say) the '500 year event' because this implies a very long period of hydrological stability (Klemeš, 1986). Secondly, in the public perception at least, a long return period tends to be equated with a much higher level of reliability than is actually the case.

There is no obvious way to avoid the problems of extrapolation in designing against extreme events, but the other aspects could be considerably improved by the adoption of time axes based on reliability rather than return periods. That is, a time axis is constructed based on some specified reliability R. Reading up the graph from N years on this axis will yield an estimate of the discharge magnitude which has a probability R of non-exceedance in N years. Regardless of the value of R, there is no necessity to extend the time-scale beyond the intended operational lifetime of the structure concerned.

It will sometimes be useful to have two reliability based time axes on a given flood plot. The first axis can be used to obtain estimates of those high flow

0022-1694/90/$03.50